

VEGF-Modified PVA/Silicone Nanofibers Enhance Islet Function Transplanted in Subcutaneous Site Followed by Device-Less Procedure

This article was published in the following Dove Press journal:
International Journal of Nanomedicine

Bin Yang^{1,*}
Guodong Cao^{1,2,*}
Kailun Cai^{1,*}
Gang Wang²
Pengping Li³
Lei Zheng¹
Haolei Cai¹
Yi Zhu¹
Xiang Li²
Yulian Wu¹

¹Department of Surgery, Second Affiliated Hospital, School of Medicine, Zhejiang University, Hangzhou, Zhejiang Province 310009, People's Republic of China; ²State Key Laboratory of Silicon Materials, School of Materials Science and Engineering, Zhejiang University, Hangzhou, 310027, People's Republic of China; ³Department of Surgery, The First People's Hospital of Xiaoshan District, Hangzhou, Zhejiang Province 310009, People's Republic of China

*These authors contributed equally to this work

Correspondence: Yulian Wu
Department of Surgery, 2nd Affiliated Hospital, School of Medicine, Zhejiang University, 88 Jiefang Road, Hangzhou, Zhejiang Province 310009, People's Republic of China
Tel/Fax +86 571 87783563
Email yulianwu@zju.edu.cn

Xiang Li
State Key Laboratory of Silicon Materials, School of Materials Science and Engineering, Zhejiang University, Hangzhou 310027, People's Republic of China
Email xiang.li@zju.edu.cn

Introduction: As heterologous islets or islet-like stem cells become optional sources for islet transplantation, the subcutaneous site appears to be an acceptable replacement of the intrahepatic site due to its graft retrievability. The device-less (DL) procedure improves the feasibility; however, some limitations such as fibrotic overgrowth or immunodeficiency still exist. Nanofibers could mimic the extracellular matrix to improve the vitality of transplanted islets. Therefore, we designed a vascular endothelial growth factor (VEGF)-modified polyvinyl alcohol (PVA)/silicone nanofiber (SiO₂-VEGF) to optimize the DL procedure.

Methods: SiO₂-VEGF nanofibers were designed by nano-spinning and characterized the physical-chemical properties before subcutaneous islet transplantation. Cell viability, vessel formation, and glucose-stimulated insulin secretion were tested in vitro to ensure biocompatibility; and blood glucose level (BGL), transplanted islet function, and epithelial-mesenchymal transition (EMT)-related biomarker expression were analyzed in vivo.

Results: The intensity of inflammatory reaction induced by SiO₂ nanofibers was between nylon and silicone, which did not bring out excessive fibrosis. The vascularization could be enhanced by VEGF functionalization both in vitro and in vivo. The BGL control was better in the DL combined with SiO₂-VEGF group. The percentage of recipients that achieved normoglycemia was higher and earlier (71% at day 57), and the intraperitoneal glucose tolerance test (IPGTT) also confirmed better islet function. The expressions of vimentin, α -SMA, and twist-1 were upregulated, which indicated that SiO₂-VEGF nanofibers might promote islet function by regulating the EMT pathway.

Discussion: In summary, our new SiO₂-VEGF combined with DL procedure might improve the feasibility of subcutaneous islet transplantation for clinical application.

Keywords: islet transplantation, subcutaneous site, VEGF modified nanofibers, device-less procedure

Introduction

Islet transplantation has become an option of type I diabetes treatment in the past decades. The site of islet transplantation can be simply divided into intrahepatic and extra-hepatic. Although intrahepatic site has higher potential of clinical application for now, several problems, such as poor islet engraftment due to the instant blood-mediated inflammatory reaction (IBMIR) and chronic islet exhaustion due to glucotoxicity, are still unresolved.¹ Furthermore, the graft rejection of intrahepatic transplantation cannot be effectively controlled² due to the islets are dispersive and deep in the liver. Therefore, the concern of extra-hepatic sites is growing.

Extra-hepatic sites include subrenal capsule, omental, intermuscular, and subcutaneous space. The subcutaneous space has been identified as an attractive option due to its accessibility, potential for imaging and retrievability.³ The main problems of subcutaneous site are the limited vascularization and low oxygen tension.⁴ Therefore, device-auxiliary and drug-auxiliary islet transplantations are designed.⁵ However, the traditional encapsulated islets still lack proper access for vascular vessels, nutrients, and growth factors.⁶ Herein, a device-less (DL) transplant procedure is reported⁵ and improved later.⁷ A silicone/nylon catheter was pre-implanted to irritate neovascularization in subcutaneous cavity, and 1 month later, the inflammatory response was terminated by removing the catheter. The islets were transplanted after catheter removal to minimize the impact of the inflammatory responses.⁸ However, there are still some limitations to this strategy. First, it is hard to control the inflammatory reaction only by manipulating the time of pre-implanted catheter because of individual differences. Second, the fibrosis is detrimental for metabolism exchange of transplanted islets, which is hard to be completely avoided. Finally, it cannot provide immune isolation which is essential for allotransplantation or xenotransplantation for future clinical application.

An ideal subcutaneous islet transplantation site should have the following advantages: (1) enough blood and oxygen supply; (2) effective metabolic exchange; (3) efficient immunoisolation of graft and host. Pre-implantation effectively enhances neovascularization and oxygen supply, while it lacks the solutions for effective metabolic exchange and immunoisolation. Recently, electrospun nanofibers have been extensively explored as scaffolds for tissue engineering because of the ability to mimic the hierarchical architecture of an extracellular matrix (ECM). It is reported that uniaxial aligned nanofibers could provide contact guidance for aligning fibroblasts and organizing ECM into a highly ordered structure.⁹ Moreover, it also presents a high surface area and high porosity with interconnectivity, which promotes cell adhesion, proliferation, and mass transport properties.¹⁰ Besides, vascular endothelial growth factor (VEGF) has been commonly used for angiogenesis stimulation and it may be especially working during early islet transplantation. As Lu S. reported, the use of VEGF in the form of modified mRNA potentially enhancing pancreatic islet function after injury.¹¹ Rachel B. Reinert also reported that normal pancreatic VEGF-A expression is much more critical for

the recruitment of endothelial cells and the subsequent stimulation of endocrine cell proliferation during islet development rather than adult islets.¹²

In this study, we designed VEGF modified PVA/SiO₂ composite nanofibers (SiO₂-VEGF) for subcutaneous islet transplantation after DL procedure. Our results suggested that SiO₂-VEGF had higher angiogenic ability than silicone and induced milder foreign body inflammatory response than nylon. This material could enhance subcutaneous transplanted islet function compared to DL procedure only and it may work via regulating EMT related cell signal pathways.

Materials and Methods

Materials

PVA (MW 85,000–124,000, Sigma-Aldrich, St. Louis, Missouri, USA), TEOS (Solarbio, Beijing, China), DMF (Solarbio), APTES (Solarbio), MES (Solarbio), EDC (1-ethyl-3-(3-dimethylaminopropyl) carbodiimide, Solarbio), NHS (N-hydroxysuccinimide, Solarbio), heparin (Solarbio), Roswell Park Memorial Institute (RPMI)-1640 medium (GIBCO BRL, Grand Island, NY, USA), β -mercaptoethanol (FD Bio, Shanghai, China), bovine serum albumin (BSA, Gibco, USA), FBS (Gibco, USA), penicillin, and Streptomycin (TBD Science, China), dimethyl sulfoxide (DMSO, Sangon, China), Matrigel (Corning, USA), Transwell (Corning, USA), Krebs–Ringer bicarbonate buffer medium (KRBB, Solarbio), D-glucose (Sigma, USA), streptozotocin (STZ, Sigma, USA), Collagenase P (Roche, USA), Histopaque (Sigma, USA), anti-CD31 antibody (HuaAN Biotechnology, Hangzhou, China), anti-IL-1 β antibody (HuaAN Biotechnology), anti-TNF- α antibody (HuaAN Biotechnology), anti-collagen I antibody (HuaAN Biotechnology), HRP-conjugated secondary antibodies (Dako, Glostrup, Denmark), HE (KeyGen Biotech, Nanjing, China), Masson (Leagene, China), 3-(4,5-dimethyl-2-thiazolyl)-2,5-diphenyl-2-H-tetrazolium bromide (MTT, Sigma, USA), VEGF Elisa Kit (Liankebio, China), rmVEGF (Peprotech, USA), AO/PI Live/Dead Detection Kit (Biolab, China), Annexin-V/PI apoptosis Detection Kit (KeyGen Biotech), Cell Cycle Detection Kit (KeyGen Biotech), Insulin Elisa Kit (Cusabio, China), annexin V/propidium iodide apoptosis detection kit (m3021-2, Molecular Biology and Chemical Company, Shanghai, China).

Fiber Synthesis

PVA/silicon nanofibers were synthesized first. Briefly, PVA was dissolved in distilled water by magnetic stirring at 70°C,

and further stirred in an oil bath at 80°C for 8 hrs (Sol A). In a separate procedure, TEOS (5 g) was then slowly added into the mixture of distilled water (5 g) and Phosphoric acid (0.1 g) and further stirred for 8 hrs at room temperature (Sol B). Sol A and B were subsequently mixed and magnetic stirred overnight at room temperature. The composite precursor was then subjected to a centrifugal spinning process in a laboratory-scale Cyclone L-1000M from Fiberio Technology Corporation to produce fine fibers. The spinneret was equipped with 30-gauge regular bevel needles (Beckett-Dickerson). 3 mL of the mixed solution was deposited in a plastic syringe with a stainless-steel needle. The needle was connected to a high-voltage generator as anode, while the cathode was connected to a fiber collector covered with a piece of aluminum foil. A voltage of 18–20 kV and a constant flow rate of 0.5 mL for 1 h were applied to the solution with the tip-to-collector distance of 20 cm. After electrospinning for 1 hr, the collected PVA/silica fiber membranes were dried in baker at 37°C overnight, and further cooled to room temperature.

Fiber Modification

Mouse VEGF was conjugated to nanofibers via EDC/NHS reaction. Briefly, 1 cm² nanofibers was added to the mixture of 40 mL DMF and 1.6 g APTES 80°C overnight. 96.5 mg MES powder was added to 90 mL ddH₂O, and then the pH value was adjusted to 5.6 by added the NaOH solution slowly. The MES solution was diluted with water to 100 mL (Sol C). Next, 0.0144 g EDC, 0.0144 NHS and 1 g heparin were added to MES solution (Sol C). Soak the NH₂- nanofibers in Sol C for 30 mins, then these nanofibers were added with slow shaking for 3 hrs. Finally, these activated nanofibers were added to the VEGF solution (concentration = 100 ng/mL) and reacted for 12 hrs in 4°C condition. The supernatant was removed by washing at least 3 times.

Nanofiber Characterizations

The as-prepared nanofibers were analyzed by TEM (transmission electron microscope H-7650; Hitachi Ltd., Tokyo, Japan), FTIR (Nicolet 5700 spectrometer, Thermo Electron Scientific Instruments Corp., Madison, WI, USA) and ZLS (Zetasizer Nano Series Instrument, Malvern). Briefly, every sample (0.5 g) was evenly placed on a carbon-coated copper grid, and then stained with 2% uranyl acetate solution. After sufficient grinding and air-drying at room temperature, the sample-loaded grid was observed under TEM. The chemical groups in different samples were characterized by FTIR of

KBr powder pressed pellets from the wavelengths of 4000 to 500 cm⁻¹. Zeta potential measurement was carried out by samples diluted in a weight percentage of 0.1%. Triplicate measurements were conducted to check for the reproducibility of the result.

Cell Culture and Animals

HUVEC cell (Human Umbilical Vein Endothelial Cells, HUVEC; The Cell Bank of Type Culture Collection of Chinese Academy of Sciences, ATCC, USA) and MIN-6 cell (Fuheng Biology, Shanghai, China), a mouse insulinoma beta cell line, were grown in regular RPMI-1640 medium supplemented with 50 ng β-mercaptoethanol, 10% FBS, 100 IU/mL penicillin, and 100 μg/mL streptomycin, at 37°C in a humidified atmosphere (5% CO₂). ICR mice were purchased from the Laboratory Animal Center of Zhejiang University (Hangzhou, China). The animals were fed in the new environment (room temperature, 20 ± 1°C; relative humidity, 55 ± 15%; 12 hrs light/12 hrs dark illumination cycle), in which food and water were provided ad libitum throughout the experiments. All the animal experiments were executed according to the ethical guidelines of the Animal Experimentation Committee in the College of Medicine, Zhejiang University, Hangzhou, People's Republic of China.

Cell Viability and Cell Apoptosis

For the cell viability/apoptosis assessment, MIN-6/HUVEC cells (3×10⁶ cells/well, in 6-well tissue culture plates) were co-cultured with suspended nanofibers (concentration=0.1mg/mL, respectively) for 24 hrs after cell stick to the bottom of the well and then gently washed with PBS for three times. The apoptosis was analyzed by FCM (BD FACSCalibur, BD Biosciences Pharmingen, San Diego, CA, USA) after incubation with Annexin V/PI apoptosis detection kit (both 5 μg/mL) at room temperature in a dark place for 15 mins.

The cytotoxicity of nanofibers in MIN-6 cell and HUVEC cell was assessed by MTT assay according to the manufacturer's protocol. MIN-6/HUVEC cells were seeded in 96-well plates at a density of 8000/5000 cells/well, respectively, with 200 μL of complete medium and incubated overnight. The culture medium was replaced with 200 μL of nanofiber suspended solution (concentration=0.1mg/mL). After being incubated for 4 hrs, the cells were cultured with normal complete DMEM again for another 19 hrs. 20 μL of MTT stock solution was added to each well and incubated for 4 hrs, and then the discarded medium and formazan crystals were dissolved with 150 μL of DMSO. Absorbance was

detected with a Microplate Reader (Bio-Rad, Hercules, CA, USA) at a wavelength of 570 nm. Blank wells with 150 μ L of DMSO were used as the internal control.

Vessel Formation Study on the Nanofibers

The nanofiber film was cut into an appropriate size to pave the bottom of the culture wells. The HUVEC cells (3×10^4 cells/well, in 24-well tissue culture plates) were moved into cell culture dishes for 24 hrs; then, the cells were digested by trypsin and PBS washing three times, AO dye was added into the wells and incubated about 15 mins away from light. The MIN-6 cells (5×10^4 cells/well, in 24-well tissue culture plates) were moved into cell culture dishes for 8 hrs, 24 hrs, and 48 hrs, respectively. Transwell test was performed in order to observe the HUVEC cells glowing into the film.

Tube formation assay was performed by coating Matrigel (10 mg/mL) on a 96-well plate. Suspended HUVECs (25×10^3) accompanied by VEGF supernatant (containing released VEGF from VEGF-modified nanofibers) or PBS as the negative control were added to each well. The plate was incubated for 18 hrs at 37°C after which AO was used for staining viable cells. Then, the tube formation was investigated with a fluorescent microscope (Olympus BX51, Olympus, Melville, NY, USA).

Glucose-Stimulated Insulin Secretion Test

MIN-6 cells with or without nanofibers were incubated in KRBB medium (1×10^5 cells/well, in 24-well culture plates) supplemented with 1% BSA, for 45 mins, respectively. Then, the media were removed, and the cells were incubated with free glucose KRBB medium, low-glucose KRBB medium (containing 2.8-mM D-glucose) or high glucose (containing 16.7-mM D-glucose) KRBB medium, supplemented with 1% BSA at 37°C for 45 mins, after which 200 μ L of supernatant from each sample was collected and analyzed by Insulin Elisa Kit. All the groups were detected three times.

Invitro Studies

Recipient mice were rendered diabetic by several times of intraperitoneal injection of STZ (50 mg/kg) between 5~7 days before transplantation. Blood samples were obtained from the tail vein to monitor blood glucose level. Animals were considered diabetic when their blood glucose levels reached a value of 15mmol/L for three consecutive daily readings.

The islet cells were harvested by methods described previously with some modification. Briefly, 4 mL of collagenase P (1mg/mL) was injected into the common bile duct of 5- to 6-week-old ICR mice. The distended pancreas was isolated and put into a 50-mL conical tube containing an additional 5-mL collagenase P solution. Then, the tube was placed in a water bath at 37°C for 10 mins with intermittent shaking for 3 times (one tube for two pancreases). The number of islets per sample was calculated in IEQ (islet equivalent quantity) following published protocol in which one IEQ represents 150 μ m. The derived tissues were purified by Histopaque, and the islet cells were cultured overnight in RPMI 1640 containing 10% FBS, in plates.

The confirmed diabetic mice were randomly assigned into 2 groups. All recipient mice were pre-vascularization by implant silicone tubes (diameter: 4 mm) for 2 weeks and then retrieved the tubes. 200 isolated islets (with or without VEGF-nanofiber wrapped) were transplanted subcutaneously.

Blood samples were obtained from the tail vein to monitor blood glucose level (BGL), and the mice body weight. Normal BGL was defined as non-fasting of less than 12 mmol/L on 2 consecutive days. An intraperitoneal glucose tolerance test was performed on recipients with normal BGL. After a 2-hr fasting, mice were injected with 3 mg/kg body weight of 50% glucose solution, then blood samples from the tail vein were obtained at 0, 30, 60, 90, and 120 mins after injection. At the end of the study, graft resection was removed to indicating normoglycemia was dependent on the islet transplant. The grafts were collected for further histological examination.

Histological Examination

The animals were sacrificed by giving an overdose of anesthesia 2 weeks after transplantation. Subcutaneous grafts were removed and fixed in 4% paraformaldehyde, embedded in paraffin, and sliced into 4- μ m thick sections. For immunohistochemistry staining, sections were deparaffinized in xylene and rehydrated in graded ethanol and antigen-retrieval with citrate buffer. After inactivation of endogenous peroxidase with 3% H_2O_2 , sections were blocked with 1% BSA and incubated with diluted primary antibodies to insulin, IL-1 β , TNF- α , ANG II, and collagen I overnight at 4°C, and then stained with HRP-conjugated secondary antibodies. Images of stained sections were captured by a light microscope (Carl Zeiss Meditec AG, Jena, Germany) and quantified by NIH Image J software.

Statistical Analysis

Quantitative data were presented as mean \pm standard deviation and analyzed by using SPSS software, version 16.0 (SPSS Inc., Chicago, IL, USA) with one-way ANOVA analysis of variance test, and Levene test was used for homogeneity of variance test. A *P*-value <0.05 was considered as significant.

Results

Synthesis and Characterization of Nanofibers and VEGF-Nanofibers

Figure 1A shows the synthesis procedure of VEGF modified nanofibers. The morphology of our nanofibers is revealed after

VEGF conjugation (SiO₂-VEGF NF, Figure 1B) by TEM and the diameter of the fibers is approximate 4–10 nm. The fluorescence microscope picture shows that the NF is porous (Figure 1C) and Figure 1D shows the NF is mat-like for cells adhere and penetration. Figure 1D shows a photograph of the SiO₂-VEGF NF film compared to 1 Yuan RMB coin, which is used for single mouse islet transplantation. The surface of SiO₂ NF is amino enriched after APTES treatment. The terminal amine group (NHS-) of SiO₂ NF and the carboxyl group of VEGF antibody are conjugated by the NHS-EDC method and further verified by following Fourier transform infrared spectroscopy assay and Zeta potential analysis. Zeta potential analysis (Figure 1E) presents VEGF conjugation

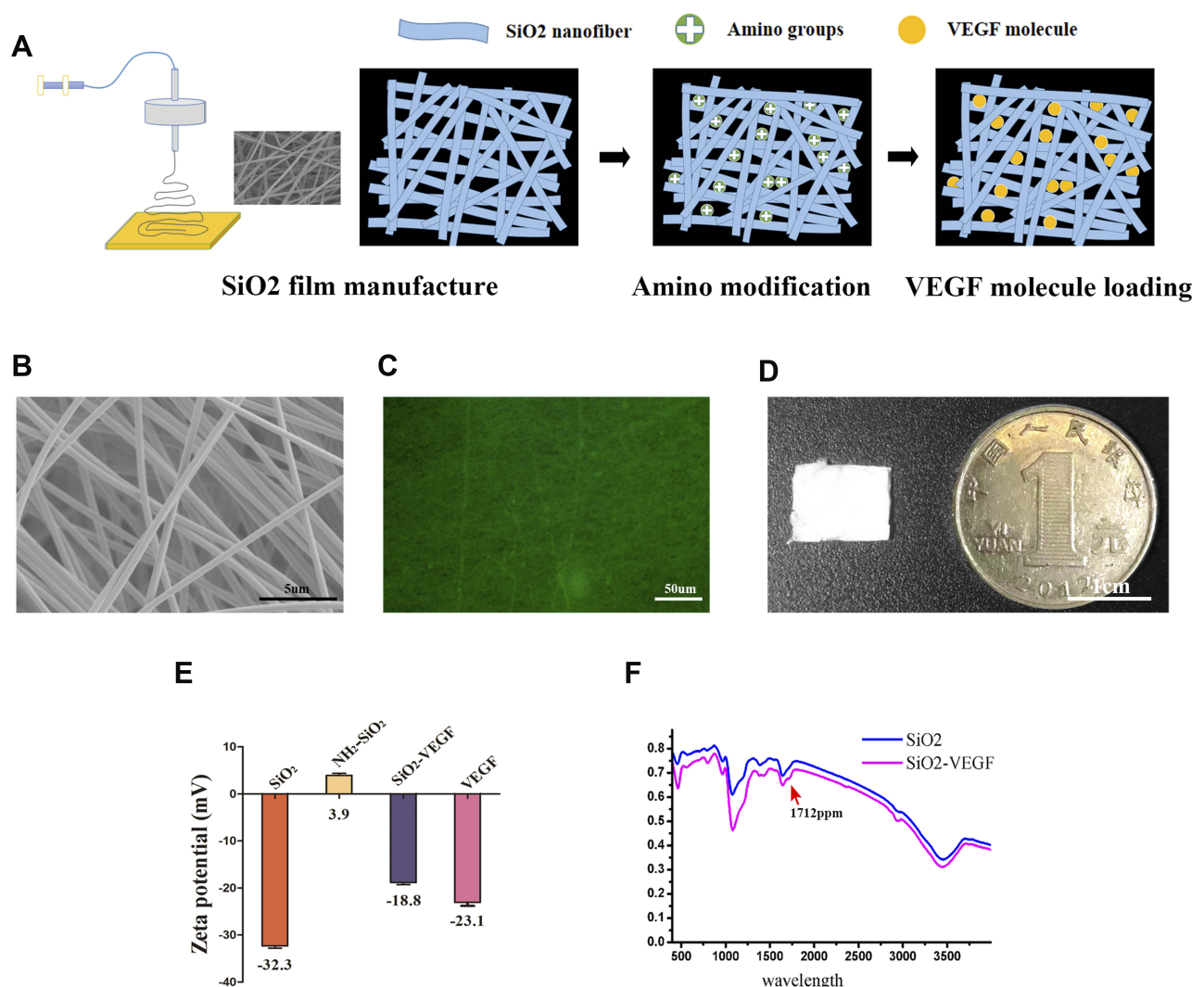


Figure 1 The morphological and physicochemical properties of the PVA/Silicone nanofibers (SiO₂ NF) and VEGF modified nanofibers (SiO₂-VEGF NF) are investigated primarily. (A). Schematic diagram of SiO₂ NF and SiO₂-VEGF NF synthesis and modification via EDC/NHS reaction. (B). Representative TEM picture of SiO₂-VEGF NF (bar = 5 μ m). (C). Fluorescence microscope picture of SiO₂-VEGF NF reveals the porous morphology of the nanofibers mat (bar = 50 μ m). (D). Illustrative diagram of SiO₂-VEGF NF mat compared to one Yuan RMB (bar = 1 cm) which is used for islet wrapping and transplantation. (E). Zeta potential assay demonstrates the stability of SiO₂, NH₂-SiO₂, SiO₂-VEGF NF and VEGF, respectively. The results indirectly demonstrate the conjugation of -NHS group and VEGF. (F). The spectrum of the SiO₂ NF and SiO₂-VEGF NF are assessed by Fourier transform infrared spectroscopic analysis. The presence of carboxyl group peak at 1712 cm⁻¹ (red arrow) in SiO₂-VEGF group indicates the carboxylation of terminal hydroxyl on the surface of SiO₂ nanofibers.

indirectly, as Zeta potential value changes through the modification. **Figure 1F** presents the VEGF-functionalize of nanofibers, the variation at 1712 ppm indicating the conjugation. We note the thickness of the nanofiber film (approximate 100–200 μm) is quite important for further graft wrapping which is controlled by spinning time (1 hr, data not shown). Over-thick film will make the pores completely intercrossed, which makes endothelial cell penetration very difficult.

Nanofibers Have No Deleterious Effect on Cell Viability and Function

The biological effects of the nanofibers are investigated first in vitro. From the variation of cell viability presented by MTT assay (MIN-6 cells (**Figure 2A**) and HUVEC cells (**Figure 2B**)), the nanofibers have no obvious deleterious effect on cell proliferation while the nanofiber concentration is up to 100 ng/mL from day 1 to day 4, which is relatively high as inorganic materials. The glucose-stimulated insulin release test further confirms that neither SiO₂ nor SiO₂-VEGF affects the function of MIN-6 cells, which still produce sufficient insulin on stimulation by high glucose (**Figure 2C**). Cell apoptosis results also confirm the nanofibers have no severe cytotoxicity (**Figure 2D**) as MIN-6 cells are labeled with suspended SiO₂ or SiO₂-VEGF for 24 hrs (100 ng/mL, respectively).

As cell cycle analyzed, the cell percentage of S and G₂ stage increase after SiO₂-VEGF NF co-culture (**Figure 2E**, blue). Tube formation assay is also performed by suspending HUVECs with SiO₂ or SiO₂-VEGF, respectively, and observed by fluorescent microscope (**Figure 2F**). As shown, HUVECs co-culture with SiO₂-VEGF forms more rings than the SiO₂ or control group. CD31 staining (**Figure 2G**) presents the endothelia cell growth on the SiO₂-VEGF group compared to the SiO₂ group (brown stain). All these results demonstrate that both SiO₂ and SiO₂-VEGF nanofibers have good biosafety to guarantee cell viability and function.

SiO₂-VEGF Nanofibers Enhance Neovascularization and Induce Mild Inflammation

The foreign body inflammation caused by SiO₂ nanofibers is moderate (**Figure 3**, lines 2 and 3, blue stain), which induces less density of neovascularization compared to nylon (**Figure 3**, line 1, brown stain). Therefore, we conjugate VEGF on nanofibers to enhance angiogenesis. As **Figure 3** indicated, the inflammatory pseudo-membrane appeared after tube pre-

implantation. Among them, nylon lead to the most chick layer and silicone is the modest (**Figure 3**, rows 1 and 2, blue stain). As CD31, IL-1 β and TNF- α stain indicated, all these materials lead to neovascularization in keeping with the intensity of inflammation. It is also found that bigger vessels formatted in SiO₂-VEGF than the SiO₂ group, while the density of the vessels has no significant difference (**Figure 3**, CD31 stain brown circle). Much more collagen deposition is found in SiO₂-VEGF than SiO₂ NF (**Figure 3**, Collagen I stain).

SiO₂-VEGF Nanofibers Enhance the Function of Islet Transplanted Subcutaneous of Diabetic Mice

Figure 4 shows the subcutaneous transplantation procedure of DL or subcutaneous SiO₂-VEGF, respectively. The blood glucose level (BGL) of all mice that received 200 IEQ islets transplanted subcutaneous decreased after islet transplantation, and the average BGL of DL combined SiO₂-VEGF group is lower (**Figure 5A**). Recipients undergo graft-rectomy 70 days post-transplantation and become diabetic again, demonstrating that normoglycemia is maintained by the islet graft before. According to BGL, the body weight of the SiO₂-VEGF group is also heavier (**Figure 5B**). The percentage of recipients achieved normoglycemia is higher and earlier as well. However, not all the recipients of DL combined SiO₂-VEGF group achieve normoglycemia after transplantation (71% (5/7) for SiO₂-VEGF NF group; 60% (3/5) for DL group, **Figure 5C**), which is better to Pepper's results (40–60%), but the persuasion is not strong enough as less data. 60 days after transplantation, an intraperitoneal glucose tolerance test (IPGTT) is performed on normoglycemic mouse recipients to test the glucose challenge response ability. All mice tested responded well, and DL combined SiO₂-VEGF group was better (**Figure 5E and D**). As **Figure 5F** insulin staining presented, both DL and DL combined SiO₂-VEGF group contains abundant insulin-positive stain cells (red arrows present the islet). The expression of CD31, IL-1 β , TNF- α , Collagen I and Massion stain is similar to **Figure 3**. Tunnel stain for cell apoptosis assay of DL or DL combined SiO₂-VEGF-treated islet grafts confirms good functional cell viability as **Figure 5G** shows.

The Expressions of Vimentin, α -SMA, Twist-1 are Upregulated by SiO₂ Nanofibers but Not E-Cad

To explore the potential mechanism, we evaluate the expression of Vimentin, Ang2, α -SMA, Twist-1, E-cad

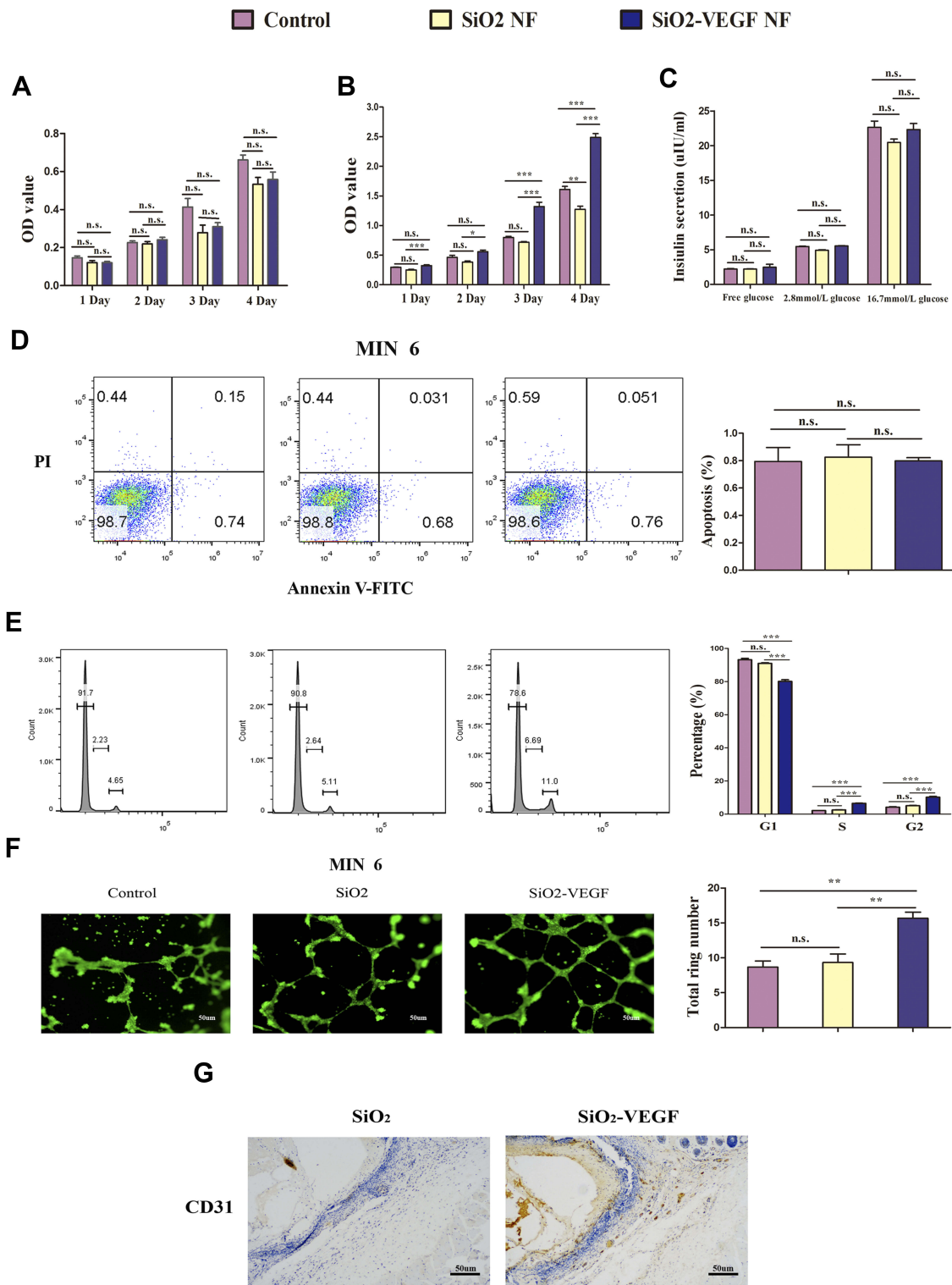


Figure 2 The biomaterial properties are tested in vitro (pink as control, yellow as SiO₂ NF, blue as SiO₂-VEGF NF). (A) MIN-6 cells and (B) HUVEC cells are cultured with SiO₂ NF or SiO₂-VEGF NF for 1–4 days and cell viability are assessed by MTT assay. Absorbance was detected with a Microplate Reader at a wavelength of 570 nm; (C) The insulin release assay of MIN-6 cells is tested after they are pre-treated with SiO₂ NF or SiO₂-VEGF NF for 24 hrs. (D) Cell apoptosis is calculated by flow cytometry, and the percentages had no significant difference among these three groups. (E) HUVEC cell cycle assay indicated the cell percentage of S/G2 increased on SiO₂-VEGF NF group for pre-cultured 24 hrs (SiO₂-VEGF group, S=6.69; G2=11.0). (F) After suspended HUVECs were treated with SiO₂-VEGF NF for 24 hrs, tube formation is observed by fluorescent microscope directly and the total ring number significantly increased. (G) CD31 staining (brown stain) verified the endothelial cell growth on SiO₂-VEGF NF group (* represents P<0.05; ** represents P<0.01; *** represents P<0.001 and ns represents no significance, respectively).

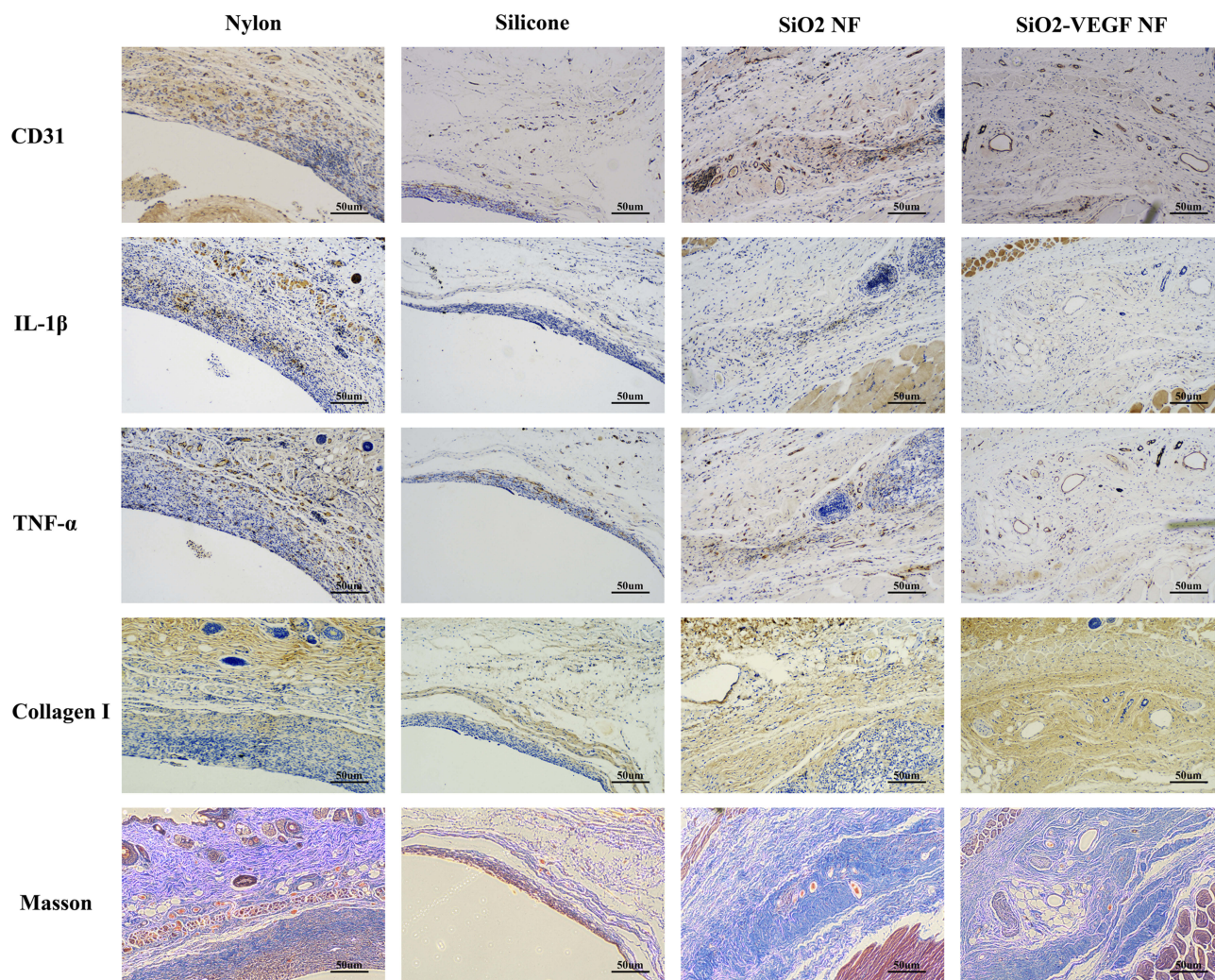


Figure 3 Representative picture of nylon, silicone, SiO₂ NF, and SiO₂-VEGF NF stained by CD31, IL-1 β , TNF- α , Collagen I, and Masson trichrome stain, respectively. As nylon (Figure 3, row 1) and silicone (Figure 3, row 2) show, nylon caused severe foreign body inflammation (IL-1 β and TNF- α), stronger vascularization (CD31), sicker collagen deposition (Collagen I), and much more fibrosis (Masson). The foreign body inflammation caused by SiO₂ NF or SiO₂-VEGF NF is moderate, which induces less density of neovascularization as nylon (Figure 3, rows 3 and 4).

by Western blot (Figure 6). We find nylon remarkably enhances Vimentin, Ang2, α -SMA, Twist-1 expression in subcutaneous surrounding tissues and there is no significant difference of E-cad expression between silicone and nylon (Figure 6A and B). Similar molecular alterations are consistent with gradient IL-1 β concentration increasing from 1ng/mL to 10ng/mL in HUVECs except Ang2 (Figure 6A and C). Next, we confirm the expression of Vimentin, α -SMA, Twist-1 and VEGF are upregulated in vitro (Figure 6D and F) and in vivo (Figure 6D and E).

Discussion

With the ongoing study of xenogeneic islets and islet stem cell transplantation, subcutaneous has become an acceptable islet transplantation site of type I diabetes because it is

retrievable for biopsy. DL procedure provides a new subcutaneous islet transplantation strategy, and the key of this method is a controllable biological pseudo-membrane formed by pre-implanted foreign body, which induces inflammatory reaction and can be conveniently ceased by removing. It is reported that hydrophilic nylon induces stronger inflammatory response than silicone and stimulates better inflammatory neovascularization which translates into more effective diabetes reversal.⁵ However, the inflammation that underlies vascularization also impairs islet function.⁸ Inflammatory cell infiltration induces and formats a fibrotic deposition around grafts, which reduces the nutrient supply and impair the cell viability.¹³ Herein, the trade-off between less inflammation and more neovascularization needs improvements. In this study, we present that the SiO₂-

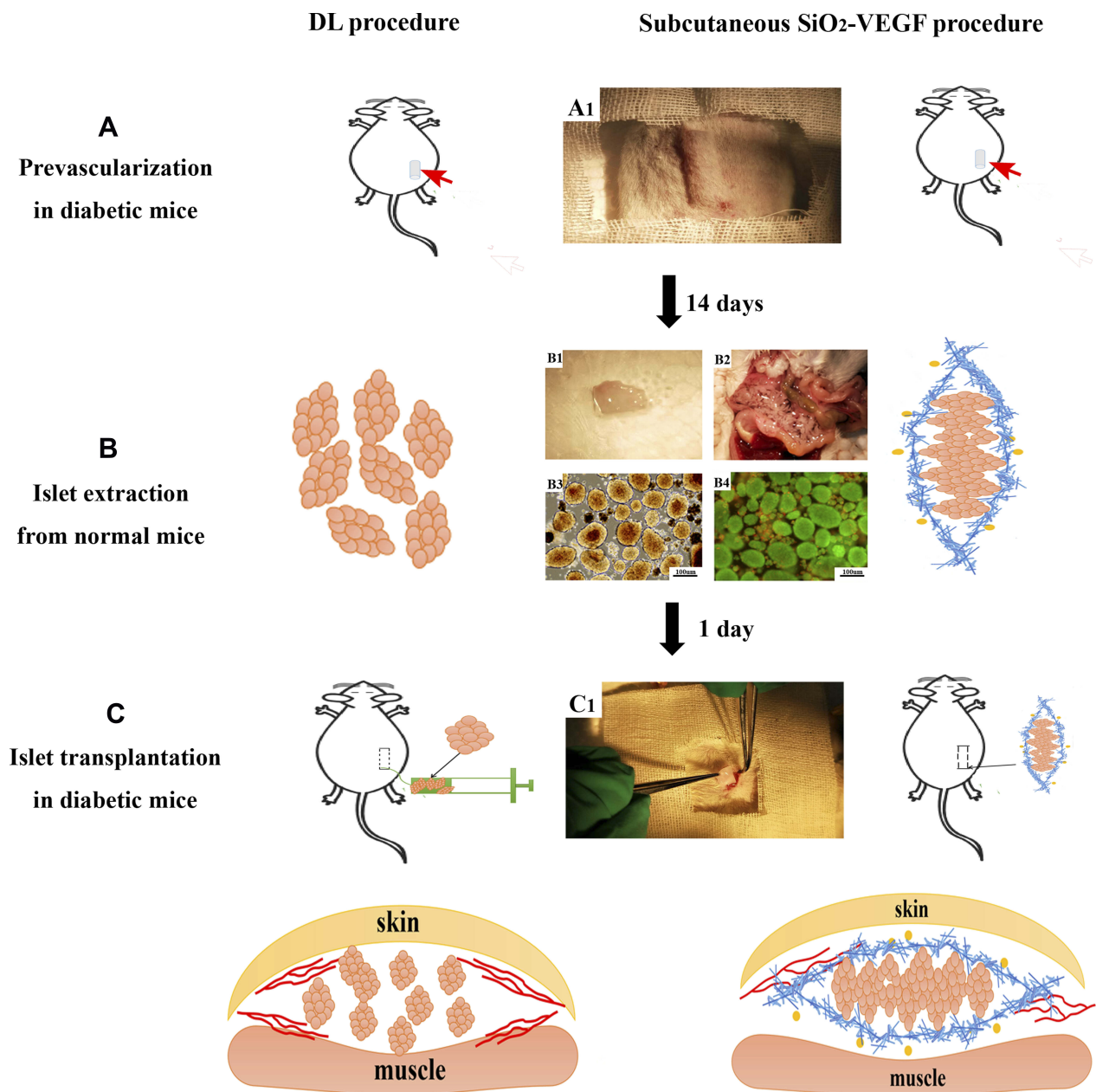


Figure 4 Schematic diagram outlining the protocol of DL or DL combined SiO₂-VEGF NF subcutaneous islet transplantation. It contains 3 steps including: **(A)** “Pre-implant the catheter (red arrow) to prevascularization and removal after 14 days. A1 presents the catheter is pre-implanted subcutaneously; **(B)** islet isolation and SiO₂-VEGF NF wrapping. Blue mat presents nanofibers wrapping and yellow dots present the VEGF on the surface of nanofibers. (B1: wrapped islets; B2: expanded mouse islet for isolation; B3: syngeneic islets are isolated and collected (bar=100 µm); B4: islet viability is detected by live/dead assay (bar=100 µm)); **(C)** islet or wrapped islet (C1) transplanted in the prevascularized (represented as red curves) percutaneous cavity.

VEGF nanofibers have modest properties between nylon and silicone as reported otherwise before. It enhances/induces the formation of new blood vessels without forming thick and dense fibrotic layer compared to nylon.

Nanofibers are prepared by electrospinning, which is an efficient technique that allows the fabrication of fibrous matrices with controllable fiber diameter and thickness.¹³ It is reported that the elongated electrospun fibers resemble

collagen fibers, form highly porous scaffolds by fibers interconnected, which mimic the architecture of ECM, allow for easy cells adherence and blood vessel growth a.¹⁴ This nano-architecture is much more controllable and convenient than nylon or silicone catheter, and it is also very suitable to rebuild islet–ECM interaction. Lots of previous islet encapsulation strategies have been failed probably due to the loss of cell–ECM interactions and biophysical cues, which make insulin-

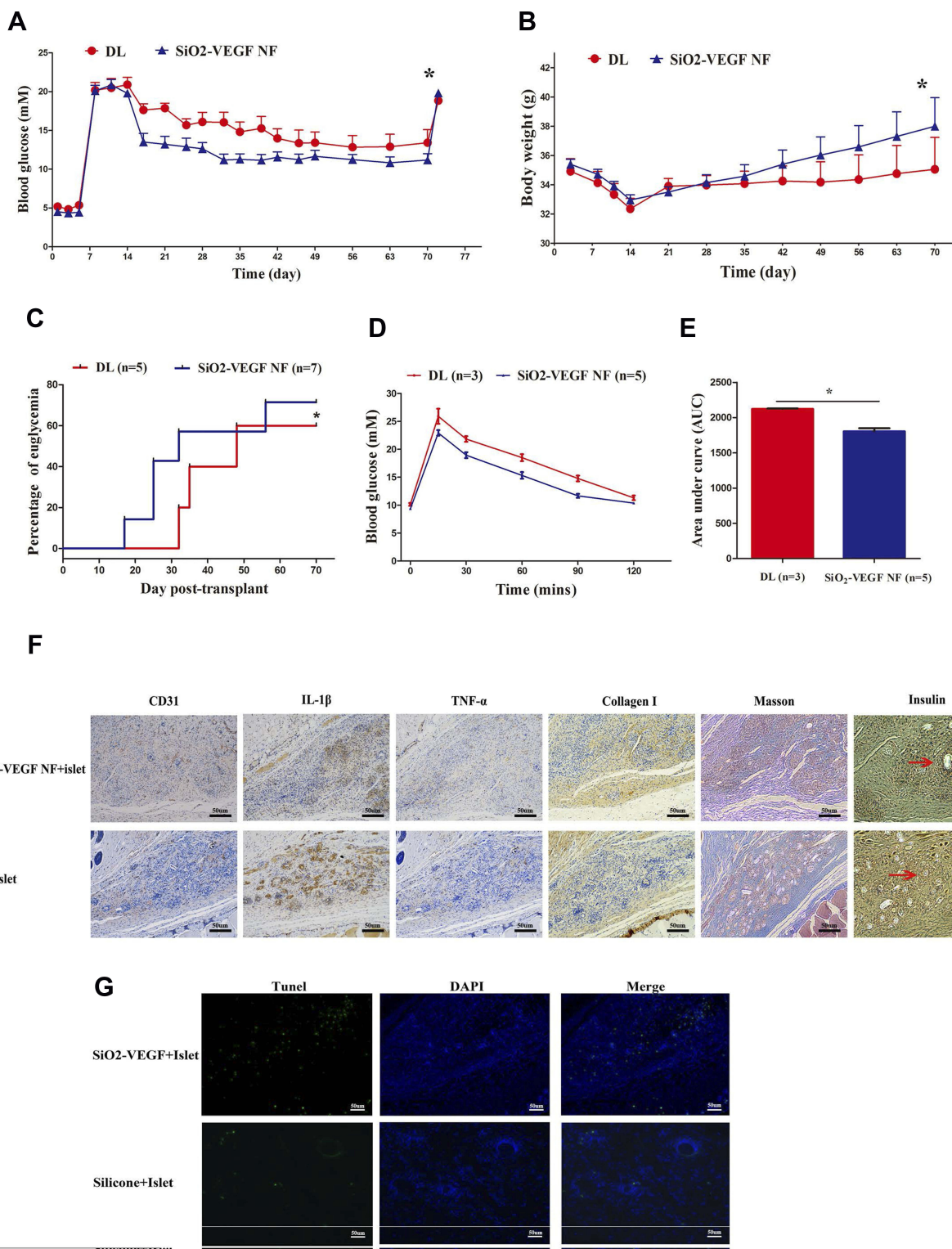


Figure 5 (A) Average blood glucose levels (BGL) of STZ-induced diabetic ICR mice before and after transplantation with 200 IEQ syngeneic islets treated with DL combined SiO₂-VEGF are lower than DL group (5 mice in each group; * represents P<0.05). (B) The average body weight of mice on SiO₂-VEGF NF group is significantly higher than those observed in mouse recipients of the same number of islets beginning at day 28 after transplantation and onward (* represents P<0.05). (C) The percentage of euglycemia mice after subcutaneous islet transplantation (3/5 in DL group; 5/7 in SiO₂-VEGF NF group; * represents P<0.05). (D, E) The BGL and AUC results of mice, which achieved euglycemia, after intraperitoneal glucose injection test at day 60 post-transplantation, respectively. (DL group, N=3; DL combined SiO₂-VEGF group, N=5; * represents P<0.05). (F) Representative immunohistochemical picture of DL or DL combined SiO₂-VEGF NF treated islet grafts, respectively. DL combined SiO₂-VEGF NF group shows relatively better vascularization (CD 31 stain), less inflammation (IL-1β and TNF-α stain) and thicker collagen deposition (collagen I stain). Brown dots reveal insulin-positive stained cells (indicated with red arrows, bar = 50 μm). (G). TUNEL stain for cell apoptosis (green dots) assay of DL or DL combined SiO₂-VEGF treated islet grafts, respectively (bar = 50 μm).

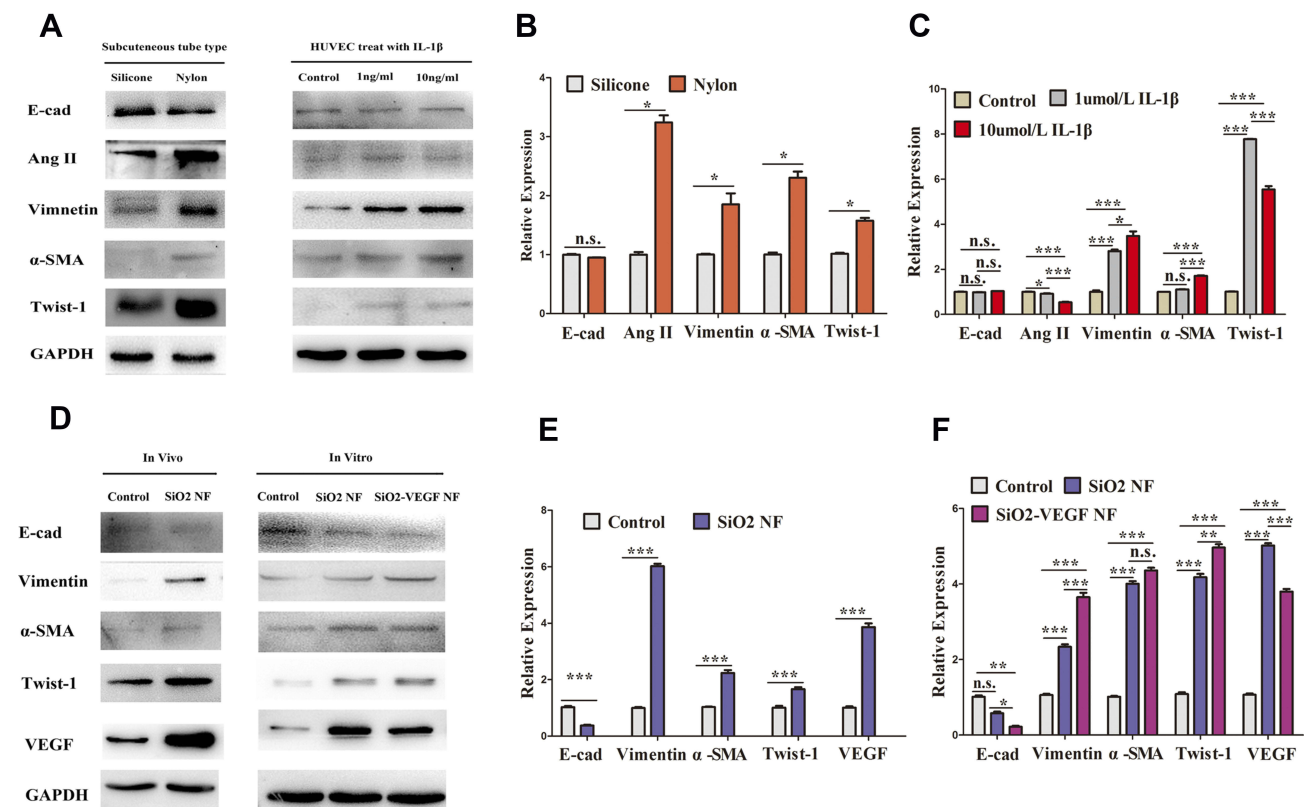


Figure 6 (A) The expression of EMT related cytokines by silicone or nylon treated tissue, and HUVEC cells treated with IL-1 β for 24 hrs by gradient increasing concentration (0, 1, 10 ng/mL) respectively. (B) the expression of E-cad, Ang2, Vimentin, α -SMA, and Twist-1 by silicone or nylon treated tissue and (C) HUVECs treated with gradient increasing IL-1 β concentration (0, 1, 10 ng/mL, respectively). (D–F) The expression of E-cad, Vimentin, α -SMA, Twist-1, and VEGF in vitro and in vivo (* represents $P < 0.05$; ** represents $P < 0.01$; *** represents $P < 0.001$ and ns represents no significance, respectively).

producing β cells undergo multiple cell death processes.^{15,16} To the aim of rebuilding cell–ECM interaction, some advances in fabrication of three-dimensional (3D) grapheme foams (GFs) are reported to afford effective cell attachment and proliferation and used for tissue regeneration as nerve, bone, cardiac, and skin.¹⁷ However, the pore size of these 3D GFs is usually between 100 and 400 μm , which is too large for islet transplantation. In our experiments, we choose PVA/silicone nanofibers because the hydrophilic nature of PVA makes it benign to living tissue and degradable via hydrolysis.¹⁸ The chemical adsorption surface modification method is used for VEGF conjugation¹⁹ as its convenience. Our results indicate that SiO₂ nanofibers could induce neovascularization as other catheters with milder inflammation compared to nylon, and in addition, SiO₂-VEGF nanofibers could further enhance the vascularization. On the other side, collagen tissues have been reported to enhance islet survival and insulin secretory function in vitro by using oligomer to encapture islets,^{20–22} which means collagen content instead of pure fibrotic encapsulation may be beneficial to re-establishing of islet matrix. In our experiments, collagen I expression around the transplanted

site increased in the SiO₂-VEGF group (Figure 3, Collagen I staining). Furthermore, nanofibers also have the capability to effectively shield the allografts from the immune attack of the host.¹³ Our results revealed less immune cells penetrate the nanofibrous layers compared to nylon (Figure 3, TNF- α stain); however, stronger evidence to confirm the contribution of collagen I enrichment needs to be studied further.

VEGF has been commonly used for angiogenesis stimulation. As Hadar pointed out, the VEGF release module concerns for vessel stimulation, which is optimal to initially release a high fraction of the loaded VEGF, as termed a “burst release”²³ and subsequently well-defined slow-release kinetics follows, in order to maintain the effect.²⁴ But they also conclude that this release kinetics is affected by many factors, including polymer swelling, biomolecular dissolution/diffusion, and biomolecule/polymer ratios.¹⁴ Therefore, it is difficult to predict the controlled release profile of an incorporated protein actually. In our study, we do find SiO₂-VEGF nanofibers stimulating tube formation (Figure 2F) in vitro and neovascularization density (Figure 3, CD31 stain) in vivo; however, the pattern of VEGF release is unclear.

Another critical and controllable condition to regulate the inflammatory pseudo-membrane is the time window of second transplantation. As Pepper reported,⁵ the pre-implanted time is 4 weeks, while some others reported that angiogenesis after transplantation is mostly generated between days 7 and 14.⁸ Our results suggest that tube pre-implanted for 14 days is suitable for completing the formation of neovascularization without forming densely inflammatory pseudo-membrane (Figure 3). Although chick fibro-layer can effectively prevent IBMIR damage during the following migration of islet cells, it is also possible to hinder the metabolic exchange between the grafts and the host circulation.

We further test some molecular biomarker expression of transplanted tissues to explore the potential mechanism of our DL combine nanofiber procedure. We find nylon enhances Vimentin, Ang2, α -SMA, Twist-1 expression in subcutaneous surrounding tissues (Figure 6A and B) and similar molecular alterations occur when gradient IL-1 β concentration increasing (Figure 6A and C). IL-1 β is a classical inflammation factor, and it is also reported to induce a significant upregulation of EMT markers.²⁵ Our results hint EMT may possibly occur after transplantation induced by foreign body or inflammation factors. It is worth to note that after IL-1 β treatment in HUVECs, the expression of Vimentin, α -SMA, Twist-1 are up-regulated except Ang2 (Figure 6C). Ang2 is a pro-angiogenic and pro-inflammatory vascular destabilizer that cooperates with VEGF.²⁶ The expression of VEGF increased in response to Ang2 overexpression and vice versa.²⁷ Compared to Figure 6F, we may infer EMT may be induced by both inflammatory and angiogenesis factors; and inflammatory factors induce less angiogenesis than released VEGF directly, which means VEGF plays a more important role to enhance neovascularization. In addition, VEGF could activate VEGFR-1 (Vascular endothelial growth factor receptor-1) and lead to an increase in expression of the EMT-associated transcription factors.²⁸ It is reported that cell apoptosis is reduced and angiogenesis of tissues is increased by increased expression of Vimentin, Twist-1, and decreased expression of E-cadherin.²⁷ EMT is also reported to induce abnormal angiogenesis²⁹ through activating the β -catenin-VEGF pathway³⁰ or Wnt/ β -catenin pathway in HUVEC cells.³¹ Besides, not only is VEGFR-1 involved in angiogenesis, it is also reported directly to contribute to tumor cell survival.³² Our HUVEC cell cycle results suggest that angiogenesis enhanced as the cell percentage of S/G2 increased after SiO₂-VEGF co-culture. These results above indicate that SiO₂-VEGF nanofibers may enhance neovascularization and islet function via EMT. Further confirming investigation as

characteristic morphologic changes of EMT, including loss of polarity, increased intercellular separation, and the presence of pseudopodia is warranted.

Conclusion

In this study, we tried SiO₂-VEGF nanofibers to improve the feasibility of DL procedure for subcutaneous islet transplantation. It was found that SiO₂-VEGF induced less foreign body inflammatory response than nylon and enhanced islet function. The expression of Vimentin, α -SMA, and Twist-1 was upregulated but not E-cad in transplanted tissues, which indicated that SiO₂-VEGF nanofibers might enhance tissue neovascularization and islet function via EMT-related cell signal pathway. The nanofibers are expected to raise the possibility of clinical subcutaneous islet transplantation.

Acknowledgments

This work was funded by the Natural Science Foundation of Zhejiang Province of China (Grant number: Q16H180002) and National Natural Science Foundation of China No.81570698 and 81702316.

Author Contributions

Bin Yang, Guodong Cao and Kailun Cai contributed equally to this work. Yulian Wu and Xiang Li are co-correspondence authors. All authors contributed to data analysis, drafting and revising the article, gave final approval of the version to be published, and agree to be accountable for all aspects of the work.

Disclosure

The authors report no conflicts of interest in this work.

References

- Bertuzzi F, De Carlis LG. Subcutaneous islet allotransplantation without immunosuppression therapy: the dream of the diabetologists and of their patients. *Transplantation*. 2018;102(3):351–352. doi:10.1097/TP.0000000000001947
- Desai T, Shea LD. Advances in islet encapsulation technologies. *Nat Rev Drug Discov*. 2017;16(5):338–350. doi:10.1038/nrd.2016.232
- Pepper AR, Pawlick R, Bruni A, et al. Harnessing the foreign body reaction in marginal mass device-less subcutaneous islet transplantation in mice. *Transplantation*. 2016;100(7):1474–1479. doi:10.1097/TP.0000000000001162
- Gamble A, Pepper AR, Bruni A, Shapiro AMJ. The journey of islet cell transplantation and future development. *Islets*. 2018;10(2):80–94. doi:10.1080/19382014.2018.1428511
- Pepper AR, Gala-Lopez B, Pawlick R, Merani S, Kin T, Shapiro AM. A prevascularized subcutaneous device-less site for islet and cellular transplantation. *Nat Biotechnol*. 2015;33(5):518–523. doi:10.1038/nbt.3211

6. Galisova A, Fabryova E, Sticova E, et al. The optimal timing for pancreatic islet transplantation into subcutaneous scaffolds assessed by multimodal imaging. *Contrast Media Mol Imaging*. 2017;2017:5418495. doi:10.1155/2017/5418495
7. Pepper AR, Bruni A, Pawlick RL, et al. Long-term function and optimization of mouse and human islet transplantation in the subcutaneous device-less site. *Islets*. 2016;8(6):186–194. doi:10.1080/19382014.2016.1253652
8. Vlahos AE, Cober N, Sefton MV. Modular tissue engineering for the vascularization of subcutaneously transplanted pancreatic islets. *Proc Natl Acad Sci U S A*. 2017;114(35):9337–9342. doi:10.1073/pnas.1619216114
9. Xue J, Xie J, Liu W, Xia Y. Electrospun nanofibers: new concepts, materials, and applications. *Acc Chem Res*. 2017;50(8):1976–1987. doi:10.1021/acs.accounts.7b00218
10. Fu Y, Li X, Ren Z, Mao C, Han G. Multifunctional electrospun nanofibers for enhancing localized cancer treatment. *Small*. 2018;14:e1801183. doi:10.1002/sml.v14.33
11. Lu S, Li J, Lui KO. Individual variation in conditional beta cell ablation mice contributes significant biases in evaluating beta cell functional recovery. *Front Endocrinol (Lausanne)*. 2017;8:242. doi:10.3389/fendo.2017.00242
12. Reinert RB, Brissova M, Shostak A, et al. Vascular endothelial growth factor-A and islet vascularization are necessary in developing, but not adult, pancreatic islets. *Diabetes*. 2013;62(12):4154–4164. doi:10.2337/db13-0071
13. Wang K, Hou WD, Wang X, et al. Overcoming foreign-body reaction through nanotopography: biocompatibility and immunoisolation properties of a nanofibrous membrane. *Biomaterials*. 2016;102:249–258. doi:10.1016/j.biomaterials.2016.06.028
14. Zigdon-Giladi H, Khutaba A, Elimelech R, Machtei EE, Srouji S. VEGF release from a polymeric nanofiber scaffold for improved angiogenesis. *J Biomed Mater Res A*. 2017;105(10):2712–2721. doi:10.1002/jbm.a.v105.10
15. de Vos P, Smink AM, Paredes G, et al. Enzymes for pancreatic islet isolation impact chemokine-production and polarization of insulin-producing beta-cells with reduced functional survival of immunoisolated rat islet-allografts as a consequence. *PLoS One*. 2016;11(1):e0147992. doi:10.1371/journal.pone.0147992
16. Irving-Rodgers HF, Choong FJ, Hummitzsch K, Parish CR, Rodgers RJ, Simeonovic CJ. Pancreatic islet basement membrane loss and remodeling after mouse islet isolation and transplantation: impact for allograft rejection. *Cell Transplant*. 2014;23(1):59–72. doi:10.3727/096368912X659880
17. Amani H, Mostafavi E, Arzaghi H, et al. Three-dimensional graphene foams: synthesis, properties, biocompatibility, biodegradability, and applications in tissue engineering. *ACS Biomater Sci Eng*. 2018;5(1):193–214. doi:10.1021/acsbomaterials.8b00658
18. Amani H, Kazerooni H, Hassanpoor H, Akbarzadeh A, Pazoki-Toroudi H. Tailoring synthetic polymeric biomaterials towards nerve tissue engineering: a review. *Artif Cells Nanomed Biotechnol*. 2019;47(1):3524–3539. doi:10.1080/21691401.2019.1639723
19. Amani H, Arzaghi H, Bayandori M, et al. Controlling cell behavior through the design of biomaterial surfaces: a focus on surface modification techniques. *Advan Mater Interfaces*. 2019;6(13):1900572. doi:10.1002/admi.v6.13
20. Stephens CH, Orr KS, Acton AJ, Tersey SA, Voytik-Harbin SL. In-situ type I oligomeric collagen macroencapsulation promotes islet longevity and function in vitro and in vivo. *Am J Physiol Endocrinol Metabol*. 2018;315(4):ajpendo.00073.2018. doi:10.1152/ajpendo.00073.2018
21. Daoud J, Petropavlovskaia M, Rosenberg L, Tabrizian M. The effect of extracellular matrix components on the preservation of human islet function in vitro. *Biomaterials*. 2010;31(7):1676–1682. doi:10.1016/j.biomaterials.2009.11.057
22. Jalili RB, Moeen Rezakhanlou A, Hosseini-Tabatabaei A, Ao Z, Warnock GL, Ghahary A. Fibroblast populated collagen matrix promotes islet survival and reduces the number of islets required for diabetes reversal. *J Cell Physiol*. 2011;226(7):1813–1819. doi:10.1002/jcp.v226.7
23. Xiao H, Brazel CS. On the importance and mechanisms of burst release in matrix-controlled drug delivery systems. *J Controlled Release*. 2001;73(2):121–136. doi:10.1016/S0168-3659(01)00248-6
24. Mario G, Gabriele G. Mathematical modelling and controlled drug delivery: matrix systems. *Curr Drug Deliv*. 2005;2(1).
25. Masola V, Carraro A, Granata S, et al. In vitro effects of interleukin (IL)-1 beta inhibition on the epithelial-to-mesenchymal transition (EMT) of renal tubular and hepatic stellate cells. *J Transl Med*. 2019;17(1):12. doi:10.1186/s12967-019-1770-1
26. Wu FT, Man S, Xu P, et al. Efficacy of co-targeting Angiopoietin-2 and the VEGF pathway in the adjuvant postsurgical setting for early breast, colorectal and renal cancers. *Cancer Res*. 2016;76:23. doi:10.1158/0008-5472.CAN-16-0888
27. Li C, Li Q, Cai Y, et al. Overexpression of angiopoietin 2 promotes the formation of oral squamous cell carcinoma by increasing epithelial-mesenchymal transition-induced angiogenesis. *Cancer Gene Ther*. 2016;23(9):295–302. doi:10.1038/cgt.2016.30
28. Yang AD, Camp ER, Fan F, et al. Vascular endothelial growth factor receptor-1 activation mediates epithelial to mesenchymal transition in human pancreatic carcinoma cells. *Cancer Res*. 2006;66(1):46–51. doi:10.1158/0008-5472.CAN-05-3086
29. Acloque H, Adams MS, Fishwick K, Bronner-Fraser M, Nieto MA. Epithelial-mesenchymal transitions: the importance of changing cell state in development and disease. *J Clin Invest*. 2009;119(6):1438–1449. doi:10.1172/JCI38019
30. Wang Z, Humphries B, Xiao H, Jiang Y, Yang C. Epithelial to mesenchymal transition in arsenic-transformed cells promotes angiogenesis through activating beta-catenin-vascular endothelial growth factor pathway. *Toxicol Appl Pharmacol*. 2013;271(1):20–29. doi:10.1016/j.taap.2013.04.018
31. Pan S, An L, Meng X, Li L, Ren F, Guan Y. MgCl₂ and ZnCl₂ promote human umbilical vein endothelial cell migration and invasion and stimulate epithelial-mesenchymal transition via the Wnt/beta-catenin pathway. *Exp Ther Med*. 2017;14(5):4663–4670. doi:10.3892/etm.2017.5144
32. Ning Q, Liu C, Hou L, et al. Vascular endothelial growth factor receptor-1 activation promotes migration and invasion of breast cancer cells through epithelial-mesenchymal transition. *PLoS ONE*. 2013;8(6):e65217. doi:10.1371/journal.pone.0065217

International Journal of Nanomedicine

Publish your work in this journal

The International Journal of Nanomedicine is an international, peer-reviewed journal focusing on the application of nanotechnology in diagnostics, therapeutics, and drug delivery systems throughout the biomedical field. This journal is indexed on PubMed Central, MedLine, CAS, SciSearch®, Current Contents®/Clinical Medicine,

Submit your manuscript here: <https://www.dovepress.com/international-journal-of-nanomedicine-journal>

Dovepress

Journal Citation Reports/Science Edition, EMBase, Scopus and the Elsevier Bibliographic databases. The manuscript management system is completely online and includes a very quick and fair peer-review system, which is all easy to use. Visit <http://www.dovepress.com/testimonials.php> to read real quotes from published authors.